

Long-Period Superlattices in Alloys. II

HIROSHI SATO AND ROBERT S. TOTH

Scientific Laboratory, Ford Motor Company, Dearborn, Michigan

(Received March 2, 1962)

A theory, which has been developed recently by the authors to explain the origin and characteristics of the long-period superlattice CuAu II, is used to explain, in a more general way, similar characteristics of long-period superlattices found in face-centered cubic alloys having compositions around the A_3B . Although there is a difference in symmetry in the atomic arrangement between the AB - and A_3B -type alloys, the application of the theory can be made in a straightforward manner. It is found that one- and two-dimensional long-period superlattices can exist in the A_3B -type alloy systems, but that a three-dimensional one should not occur. In the case of the one-dimensional long-period superlattices, the theory can be reduced to the same form as for the CuAu II (AB type) case. The theory predicts correctly the period of the superlattice, e.g., those found in the Cu-Pd, Cu-Pt, Au-Cd, Ag-Mg, and Au-Zn systems, the type of antiphase, the direction of the period and the sign of the tetragonal distortion which occurs when the long-period superlattice is formed.

The theory is also applied to the case of the two-dimensional superlattice, examples of which are found in the Cu-Pd, Au-Mn, and Au-Zn alloys. Since a more detailed knowledge of the electronic structure of the alloys is necessary in dealing with the two-dimensional superlattices, less quantitative information on their characteristics is obtained. However, predictions concerning the period of the structure, type of antiphase, and lattice distortion are reasonably good.

An explanation is given for the possible relation between the magnitude of the truncation factor and the shape of the Fermi surface which is based on recent findings in the noble metals.

I. INTRODUCTION

LONG-PERIOD superlattices, a superstructure having regular antiphase domains, have been found in many alloy systems and considerable data concerning the structure of these alloys have been accumulated. In an attempt to understand the origin of the formation of such a peculiar structure we have been engaging in a systematic study, both experimental and theoretical of these alloys. In a previous paper,¹ hereafter referred to as LPS I, experimental work was reported in which additional elements in various quantities were added to the antiphase structure CuAu II. The effect of the additional elements on the period of the antiphase structure was determined, and it was found that there existed a definite relation between the period of the antiphase and the electron-atom ratio of the resulting alloy. On the basis of this observation and its analysis a theory was proposed, based upon the concept of the stabilization of alloy phases at the Brillouin-zone boundary, to explain the dependence of the period $2M$ on the electron-atom ratio e/a . This dependence is shown by the formula

$$\frac{e}{a} = \frac{\pi}{12} \frac{1}{t^3} \left(2 \pm \frac{1}{M} + \frac{1}{4M^2} \right)^{\frac{2}{3}}, \quad (1)$$

where t is a truncation factor which takes into account the nonsphericity of the Fermi surface. The above equation using the plus sign and a t value of 0.95 predicts the variation of M with e/a with considerable quantitative success for the case of CuAu II with additional elements. The equation, however, should be regarded as representing the zeroth approximation in the determination of the domain size, since other factors such

as the antiphase domain boundary energy, etc., will affect the domain size. The theory also explains why a distortion occurs in the lattice when the antiphase structure is formed. By taking into consideration the antiphase boundary energy, the theory also can explain the change in domain size with composition which occurs without a change in the e/a ratio (the concentration effect), the change in domain size which occurs with a change in temperature, and why the phase change CuAu I—CuAu II should occur (temperature effect).

In taking a composite picture of this basically order-disorder problem, it was emphasized that the main ordering energy is still due to the short-range interactions. The main feature of the proposed theory was to show that a small change in energy due to a lowering of the energy of the electrons at the Brillouin zone boundaries is sufficient to cause the formation of the antiphase structures.

The agreement between theory and experiment for the case of CuAu II is so good that one could assume that the model adopted is indeed the correct explanation for the formation of the antiphase structure in this alloy system. However, CuAu II is rather a special example of these types of alloys. In the case of CuAu II, the long-period superlattice appears at an equal composition range of A and B atoms and the symmetry of the atomic arrangement on the crystal lattice is tetragonal. On the other hand, most of the long-period superlattices have been observed at the composition near A_3B and the symmetry of the atomic distribution remains cubic. In addition to the one-dimensional periodic structures like CuAu II, two-dimensional structures have also been found. However, these alloys have basic characteristics which are common with CuAu II, and the theory adopted there is a general one. Therefore, we can expect that this type of theory should provide a

¹ H. Sato and R. S. Toth, Phys. Rev. **124**, 1833 (1961).

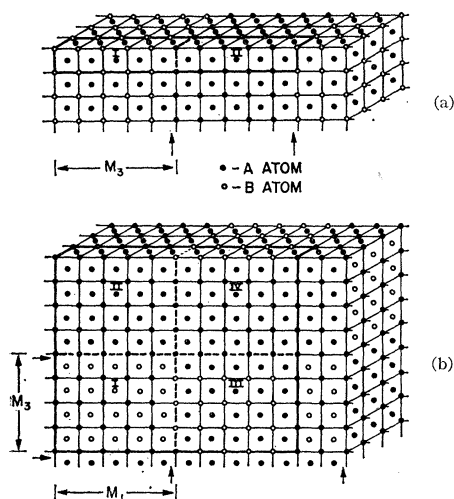


FIG. 1. One- and two-dimensional long-period superlattices in an A_3B alloy. M_1 and M_3 denote the domain size in each direction, and the arrows show the regions of the antiphase boundaries. (a) The unit cell of the one-dimensional superlattice is indicated by the dark lines, and is composed of two antiphase domains I and II of size $M_3=5.0$. (b) The unit cell of a two-dimensional superlattice is composed of four domains as indicated by the dark lines with domain sizes of $M_1=5.0$ and $M_3=4.0$.

good explanation of the characteristics of other alloys as well. The purpose of this paper is to treat the problem, especially that of the A_3B -type alloys, from a more general view than before and to compare the theoretical predictions with available experimental data.

II. SOME FEATURES OF LONG-PERIOD SUPERLATTICES

Before applying the theory to specific alloy series, it may be worthwhile to outline briefly what features of long-period superlattices should be explained by the theory, and what general experimental data is available.

Thus far, the long-period superlattice has been found mostly in face-centered cubic alloys having compositions around the AB and A_3B .² In these, only one-dimensional antiphase structures are found in the AB type while both one- and two-dimensional structures are found in the A_3B type. No three-dimensional antiphase structures have been found. By a one-dimensional antiphase structure, we mean the superperiod exists only in one direction in any particular region of the crystal. Therefore, we can describe this structure by using a long unit cell composed of a row of fundamental unit cells of the face-centered cubic lattice, in a direction of the period, with two antiphase domains of size M_3a_3 , each separated by an antiphase domain boundary as shown in Fig. 1(a). $2M_3$ is called the period of the one-dimensional long-period superlattice. For the two-dimensional case, we can describe the structure as an

² L. Guttman, *Solid State Physics*, edited by F. Seitz and D. Turnbull (Academic Press Inc., New York, 1956), Vol. 3, p. 146. Some periodic structures in hexagonal close packed systems have also been reported. See reference 13.

orthorhombic unit cell which is one unit cell thick in one direction but in the plane perpendicular to that direction includes four antiphase domains of size $M_1a_1 \times M_3a_3$ each separated by antiphase boundaries, respectively [Fig. 1(b)]. The important feature is that, as is understood from the figure, the two-dimensional periodic structure is not a simple superposition of a one-dimensional periodic structure in two directions but that the antiphase domains in two directions are connected by a definite relation. That is, the nature of the antiphase relation between I and II and that between III and IV should be the same. Furthermore, the same is true for I and III and for II and IV. A three-dimensional structure would then be described by an orthorhombic unit cell with eight antiphase domains. In the following arguments, we assume the period M_1, M_2 , etc., to be integers. The meaning of the nonintegral values of M_1, M_2 , etc., observed experimentally has been discussed in LPS I.

In forming an antiphase structure in a binary alloy with face-centered-cubic structure, two types of "out-of-step" may occur at the boundary, these being referred to as either the "first or second kind".³ An antiphase may be produced by replacing a B site by an A site. Since the face-centered-cubic structure is composed

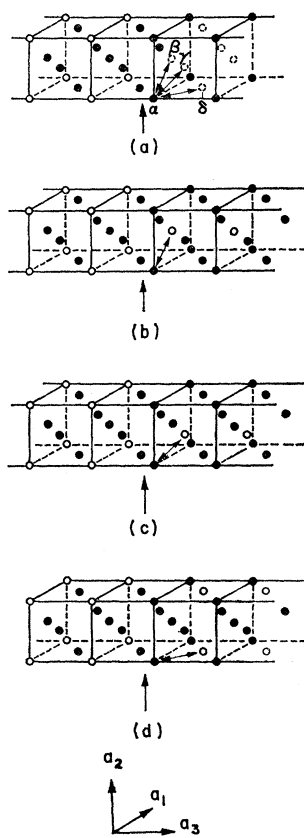


FIG. 2. Types of antiphase at a domain boundary. (a) Three different ways of exchanging sites to form an antiphase. This exchange is conveniently represented by three "out-of-step" vectors: (b) $\alpha \leftrightarrow \beta$; $\pm \frac{1}{2}(\mathbf{a}_1 \pm \mathbf{a}_2)$ antiphase of the 1st kind. (c) $\alpha \leftrightarrow \gamma$; $\pm \frac{1}{2}(\mathbf{a}_2 \pm \mathbf{a}_3)$ antiphase of the 2nd kind. (d) $\alpha \leftrightarrow \delta$; $\pm \frac{1}{2}(\mathbf{a}_1 \pm \mathbf{a}_3)$ antiphase of the 2nd kind. If an additional superperiod exists in the \mathbf{a}_1 direction (c) indicates the e type and (d) indicates the i type. The arrows at the bottom of each figure show the regions of the antiphase boundaries.

³ D. Watanabe and S. Ogawa, *J. Phys. Soc. Japan* 11, 226 (1956).

of four independent simple cubic sublattices, there are three ways of having an antiphase. Let us express the three cubic lattice vectors which are mutually perpendicular as \mathbf{a}_1 , \mathbf{a}_2 , and \mathbf{a}_3 and let the direction perpendicular to the antiphase boundary be colinear with \mathbf{a}_3 . Then the out-of-step vectors, corresponding to the replacements of the sublattices at the antiphase boundary, are $\frac{1}{2}(\mathbf{a}_1 + \mathbf{a}_2)$, $\frac{1}{2}(\mathbf{a}_2 + \mathbf{a}_3)$ and $\frac{1}{2}(\mathbf{a}_1 + \mathbf{a}_3)$. The one vector $\frac{1}{2}(\mathbf{a}_1 + \mathbf{a}_2)$ lies in the plane of the antiphase boundary and this antiphase is referred to as an antiphase of the first kind. When the out-of-step vector lies outside the antiphase boundary, it has been called an antiphase of the second kind. The two vectors for the second kind antiphase are equivalent in the one-dimensional case but can be different in the two-dimensional case. Since the difference arises when the superperiods exist in two directions, it is natural to define the difference with respect to these two axes. Let the direction of the second period be colinear with \mathbf{a}_1 . Of the out-of-step vectors for the antiphase boundary perpendicular to \mathbf{a}_3 , $\frac{1}{2}(\mathbf{a}_1 + \mathbf{a}_3)$ includes both vectors indicating two periods, but $\frac{1}{2}(\mathbf{a}_2 + \mathbf{a}_3)$ does not include the vector collinear with the direction of the other period. For future application, let us define the former as the *i* type and the latter as the *e* type. These relations concerning antiphases are illustrated in Fig. 2. The direction of the period, or the direction of the normal to the antiphase boundary, can be in any direction. However, in all cases we will be dealing with, the direction of the superperiod coincides with one of the $[100]$ directions and the antiphase boundary coincides with one of the $\{100\}$ planes as illustrated above. This fact, however, should be explained by the theory.

Experimentally, it has been found that *all* one-dimensional long-period superlattices have an antiphase of the first kind. Two-dimensional long-period superlattices have an antiphase structure which can be either the same or different in nature in the two directions. Both the first and second kind of antiphases are found to exist. It is important to explain why each superlattice chooses its particular antiphase structure.

Another distinctive feature of the long-period superlattices is the distortion which occurs as a result of its formation. In both the AB and A_3B type structures, the distortion takes place in the direction perpendicular to the antiphase boundary. This distortion, which depends upon the electron-atom ratio, should be predicted.

III. ONE-DIMENSIONAL LONG-PERIOD SUPERLATTICE

A. AB -Type Alloys

1. *Cu-Au System*

Thus far, the only good example of a one-dimensional long-period superlattice in an AB -type alloy is the alloy CuAu II ,⁴ which has been discussed fully in LPS I. A

⁴ C. H. Johansson and J. O. Linde; *Ann. Phys.* **25**, 1 (1936).

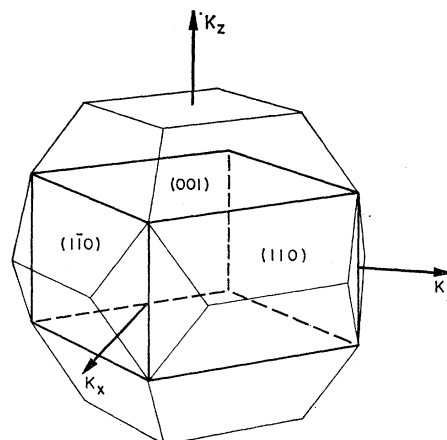


FIG. 3. Brillouin zone structure for CuAu. Thin lines represent the zone for the disordered phase; thick lines represent the zone for the ordered CuAu I phase.

brief review of this alloy is necessary here since it represents this particular class of antiphase structure.

In the ordered CuAu alloy (CuAu I type), the symmetry of the atomic distributions becomes tetragonal, and hence the Brillouin zone is anisotropic with regard to the cubic axes. The first Brillouin zone for the ordered structure is bounded by $\{001\}$ and $\{110\}$ faces as shown in Fig. 3, and can include one electron per atom. The distance from the center of the zone to the $\{001\}$ faces is much shorter than the distance to the $\{110\}$ faces and hence the Fermi surface overlaps freely in the *c* direction. Therefore, only the $\{110\}$ planes play an important role in the stabilization of the long period superlattice. The adjustment of these planes in such a way that the resulting zone just includes the Fermi surface can be done by forming a superperiod in only one direction. In Fig. 3, this is taken in the \mathbf{k}_y direction, since the \mathbf{k}_z direction is taken as the *c* axis of the tetragonal structure of CuAu I as was explained in LPS I. The accommodation of the Fermi surface and, hence, the nature of the stabilization at the zone boundaries is shown in Fig. 4.⁵ Thus the establishment of the one-dimensional antiphase structure is the unique way to stabilize a face-centered cubic AB -type ordered alloy as CuAu. Hence, it is natural to have a one-dimensional antiphase structure but not a two-dimensional one. The degree of separation of the zone boundaries depends on the size of the Fermi sphere and hence on the number of electrons. This relation between the domain size and the electron-atom ratio of CuAu II with additional elements, is given by Eq. 1, with the plus sign and a truncation factor $t=0.95$.

The explanation of why an antiphase of the first kind is found in this type of alloy is trivial. For CuAu, two

⁵ In LPS I, this figure was shown along with the (100) spots in order to indicate the location of the zone boundaries. Since the (100) spots do not exist in the reciprocal lattice of CuAu II except those of the (001) , we are now afraid that this addition of the (100) spots might have caused some confusion and misunderstandings.

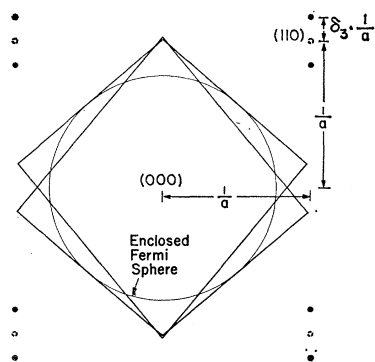


FIG. 4. Reciprocal lattice of CuAu II in a plane through the origin and parallel to the (001) plane, showing the structure of the Brillouin zone of CuAu II and of the enclosed Fermi sphere.

of the four sublattices are occupied by Cu atoms and the remaining two are occupied by Au atoms. However, there are only two equivalent sites in the lattice, and consequently an antiphase of the first and second kind as defined by the out-of-step vectors are equivalent in this particular case. There is no need to differentiate between the type of antiphase, and one can say that CuAu II is composed of antiphase boundaries of the first kind.

The distortion to be found in this type of structure has also been fully discussed in LPS I. There it was shown that a distortion in the direction of the long period of the superlattice is to be expected for the condition where the Fermi surface can be more closely accommodated due to a small distortion of the zone along the axis parallel to the long period. As a result, it is concluded that for alloy systems where the electron-atom ratio is greater than the critical value $(e/a)_c$, one expects an elongation in the direction of the superperiod. On the other hand, for systems in which the e/a ratio is less than the critical value, a contraction should occur in the direction of the period.

A long-period superlattice structure similar to CuAu II has been suggested for Mg-In alloys near the stoichiometric proportion.⁶ However, detailed results have not been reported and it is impossible to compare the data with the theory.

B. A_3B -Type Alloys

One-dimensional long-period superlattices have been found in face-centered cubic alloys of the A_3B type. The extension of the theory to this type of alloy is somewhat different from that applied to the AB type as can be seen by comparing the Brillouin zones of these structures. The Brillouin zone for the A_3B -type face-centered-cubic alloy is shown in Fig. 5. For the disordered state, the Brillouin zone is a truncated octahedron and is indicated by the thin lines in Fig. 3. When the alloy becomes ordered, the Brillouin zone splits and the first Brillouin zone is now bounded by $\{100\}$ planes, as shown in Fig. 5(a). The volume of this zone is $1/a^3$ and can accommodate only 0.5 electrons per atom. Thus, this

⁶ G. V. Raynor, Trans. Faraday Soc. 44, 15 (1948).

zone should be completely filled and should not play an important role in the stabilization of the alloy. The second Brillouin zone is bounded by $\{110\}$ planes and forms a rhombic dodecahedron, as shown in Fig. 5(b). This zone can accommodate one electron per atom and thus the surface should play an important role in the stabilization of these alloys. Stabilization can be obtained by accommodating the Fermi surface by a similar adjustment of any of the twelve $\{110\}$ surfaces as compared to the four $\{110\}$ surfaces in the AB -type alloy. It will be shown that a superperiod in one direction affects eight of the twelve surfaces, and that all twelve surfaces are affected as a result of the formation of a two-dimensional long-period superlattice. This will explain the formation of the two-dimensional superlattice and also explain why a three-dimensional long-period superlattice should not form.^{6a} The stabilization of the long-period superlattice for the A_3B -type alloy is connected with the type of out-of-step formed at the antiphase boundary. Therefore, it is expedient to discuss these two problems simultaneously.

As mentioned previously, an antiphase of the first kind is characterized by an out-of-step vector $\frac{1}{2}(\mathbf{a}_1 + \mathbf{a}_2)$ in the plane of the boundary when the superperiod is in the \mathbf{a}_3 direction, while the antiphase of the second kind is represented by a vector $\frac{1}{2}(\mathbf{a}_2 + \mathbf{a}_3)$ or $\frac{1}{2}(\mathbf{a}_3 + \mathbf{a}_1)$ outside of the antiphase boundary, these two vectors being equivalent in the one-dimensional case. The difference in the two kinds of antiphase for the A_3B alloy may be indicated by the manner of separation of the superlattice spots, and the basis for the calculation of the separation of the superlattice spots caused by the existence of a superperiod is given as follows:

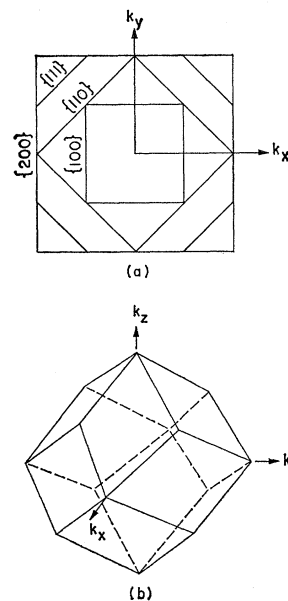


FIG. 5. Brillouin zones for an ordered A_3B alloy. (a) Brillouin zone boundaries in k_x - k_y plane. (b) Rhombic dodecahedron formed by twelve $\{110\}$ planes.

^{6a} Exceptions from this statement may be conceivable, cf. Figs. 14 and 16. Occurrence of a three dimensional superlattice, however, is still improbable. See Part IV.

The structure amplitude S for the one-dimensional long-period superlattice shown in Fig. 1(a), can be formulated in the following equation:⁷⁻⁹

$$|S| = \left| \frac{\sin \pi N_1 A_1}{\sin \pi A_1} \right| \left| \frac{\sin \pi N_2 A_2}{\sin \pi A_2} \right| \left| \frac{\sin \pi N_3 (2M_3) A_3}{\sin \pi (2M_3) A_3} \right| \times \left| \frac{\sin \pi M_3 A_3}{\sin \pi A_3} \right| |\Phi|, \quad (2)$$

where $\Phi = \Phi_I + \Phi_{II} e^{2\pi i M_3 A_3}$. A_1, A_2 and A_3 are continuous variables in the reciprocal lattice; N_3 is one-half the number of antiphase domains along the z direction and is assumed to be far larger than M_3 ; N_1 and N_2 are the numbers of unit cells along the $x(\mathbf{a}_1)$ and $y(\mathbf{a}_2)$ direction. Φ_I and Φ_{II} are the structure factors of the fundamental face-centered cubic unit cell included in the antiphase domains I and II, respectively. The relation between Φ_I and Φ_{II} is, therefore, determined by the type of antiphase between these two domains. In an A_3B -type face-centered cubic alloy with a first kind of antiphase with the long period in the $z(\mathbf{a}_3)$ -direction, Φ_I and Φ_{II} are defined in the following way:

$$\begin{aligned} \Phi_I &= E_A \{1 + \exp \pi i (A_1 + A_2) + \exp \pi i (A_2 + A_3)\} \\ &\quad + E_B \exp \pi i (A_3 + A_1), \\ \Phi_{II} &= E_A \{1 + \exp \pi i (A_1 + A_2) + \exp \pi i (A_3 + A_1)\} \\ &\quad + E_B \exp \pi i (A_2 + A_3). \end{aligned} \quad (3)$$

Here, E_A and E_B are the atomic scattering factors for electrons by A and B atoms, respectively. The manner of separation is calculated on the basis of the intensity distribution given by formulas (2) and (3). However, the approximate manner of the separation can be determined by the last structure factor Φ . Then, it is easily understood that only superlattice reflections of indices with certain mixed integers h_1, h_2 , and h_3 , depending upon the particular type of antiphase, split along the direction of the period. For example, when the direction of the superperiod is in the \mathbf{h}_3 direction and the out-of-step vector is defined by $\frac{1}{2}(\mathbf{a}_1 + \mathbf{a}_2)$ [i.e., the first kind for which Eqs. (2) and (3) were developed], those superlattice reflections with mixed h_1 and h_2 split along the $[00h_3]$ direction. Let us show this situation with the (101) superlattice spot for the sake of simplicity. By putting $A_1=1, A_2=0$ and $A_3=1$ in Eq. (3), we find

$$\begin{aligned} \Phi_I &= -E_A + E_B, \\ \Phi_{II} &= E_A - E_B, \\ |\Phi| &= |\Phi_I + \Phi_{II} e^{2\pi i M_3}| \\ &= |(E_A - E_B)| |2(1 - \cos 2\pi M_3)|. \end{aligned} \quad (4)$$

Therefore, the spot vanishes at the center (101),

⁷ S. Ogawa and D. Watanabe, *J. Phys. Soc. Japan* **9**, 475 (1954).
⁸ H. Raether, *Handbuch der Physik*, edited by S. Flügge (Springer-Verlag, Berlin, 1957), Vol. 32, pl 443.
⁹ A. B. Glossop and D. W. Pashley, *Proc. Roy. Soc. (London)* **A250**, 132 (1959).

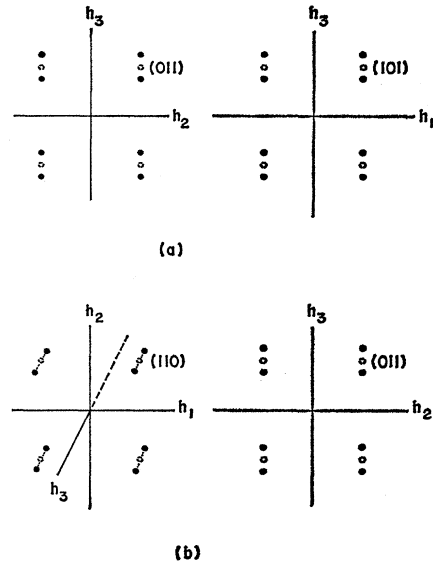


Fig. 6. Splitting of the (110) superlattice spots due to the existence of the superperiod in the \mathbf{a}_3 direction with (a) antiphase of the first kind and (b) antiphase of the second kind. The third axis is added when it is necessary to show the separation in the direction perpendicular to the plane.

meaning that a splitting of the spot occurs. The separation can be calculated to a good approximation, if M_3 is reasonably large, by

$$|\Phi| = |(E_A - E_B)| |2[1 - \cos 2\pi M_3(1 + \delta_3)]|, \quad (5)$$

since the phase factor in Φ_I and Φ_{II} does not change very much by the separation. The equation has a maximum at

$$\delta_3 = \pm n_3 / 2M_3, \quad (6)$$

where n_3 is an odd integer. Therefore, if we take the primary reflection, $n_3=1$, the spot (101) splits into two $(1, 0, 1 \pm 1/2M_3)$. It is also easily shown that if h_1 and h_2 are unmixed, S does not vanish for such superlattice spots. In this way, the manner of separation of the spots is determined.

Let us assume that the direction of the superperiod is again in the \mathbf{h}_3 direction (i.e., collinear with the \mathbf{a}_3 direction). The mode of separation of the $\{110\}$ superlattice spots for the two types of antiphase structure is shown in Fig. 6. The splitting of the $\{110\}$ spots in the reciprocal lattice for the antiphase of the first kind occurs in the \mathbf{h}_2 - \mathbf{h}_3 plane and the \mathbf{h}_3 - \mathbf{h}_1 plane, the spots being split are the $\{011\}$ and $\{101\}$ groups. The manner of separation of the spots of each group is identical to that which occurs for the case of CuAu II. Since two groups of superlattice spots split for the A_3B -type superlattice and the related Brillouin-zone boundaries are found from these spots,¹⁰ there will occur a corresponding separation on eight faces of the Brillouin zone instead of the four for the AB case. If we denote

¹⁰ N. F. Mott and H. Jones, *The Theory of the Properties of Metals and Alloys* (Clarendon Press, Oxford, 1936), p. 152.

the separation of the superlattice spots as δ_3 (which was defined in LPS I as x) then the distance from the origin of the zone to the separated zone surfaces is given by

$$(2 \pm 2\delta_3 + \delta_3^2)^{\frac{1}{2}}, \quad (7)$$

where the plus and minus signs refer to the outer and inner faces, respectively. Thus the inscribed sphere would fit uniformly within these eight Brillouin-zone faces and the reduction in the energy of electrons should take place at these faces.

If an antiphase of the second kind occurred, the out-of-step vector could be taken as the $\frac{1}{2}(\mathbf{a}_1 + \mathbf{a}_3)$. Then the superlattice spots would split in the \mathbf{h}_3 direction again but the separation would occur in the $\mathbf{h}_1 - \mathbf{h}_2$ and $\mathbf{h}_2 - \mathbf{h}_3$ planes. The manner of splitting of the superlattice spots in the $\mathbf{h}_2 - \mathbf{h}_3$ plane is the same as above, and the distance from the origin to the zone boundaries that are formed is given by Eq. (7). In the $\mathbf{h}_1 - \mathbf{h}_2$ plane, however, the separation of the spots is perpendicular to the plane and in the \mathbf{h}_3 direction. For this kind of separation, the distance from the origin of the zone to the corresponding separated faces of the Brillouin zone is given by

$$(2 + \delta_3^2)^{\frac{1}{2}} \quad (8)$$

and is different from that which occurs for the $\mathbf{h}_2 - \mathbf{h}_3$ plane. Thus the Fermi sphere cannot fit uniformly within the boundaries of this Brillouin zone, and the condition for stabilization for the second-type antiphase is definitely unfavorable compared to that which occurs for an antiphase of the first kind. Consequently, an antiphase of the first kind should occur when a one-dimensional long-period superlattice is formed, as substantiated by the experimental evidence, and stabilization will occur at eight of the twelve faces of the Brillouin zone. In order that the maximum adjustment can be achieved by the minimum separation of the spot, or by the introduction of the minimum number of antiphase boundaries, the direction of the separation of the spot should be in one of the $[100]$ directions as is easily understood from the shape of the Brillouin zone. In other words, the direction of the superperiod is always chosen to be in one of the $[100]$ directions. This explains the fact that the antiphase boundaries are always chosen to be one of the $\{100\}$ planes as stated before.

We may now compare the above predictions of the theory with the available experimental results on alloys which form a one-dimensional long-period superlattice. From Eq. (7), and as explained in LPS I, the relation between the electron-atom ratio and the domain size is given by

$$\frac{e}{a} = \frac{\pi}{12} \frac{1}{f^3} (2 \pm 2\delta_3 + \delta_3^2)^{\frac{3}{2}}, \quad (9)$$

where the domain size $M_3 = 1/2\delta_3$ and the plus and minus sign refers to stabilization at the outer- and inner-zone

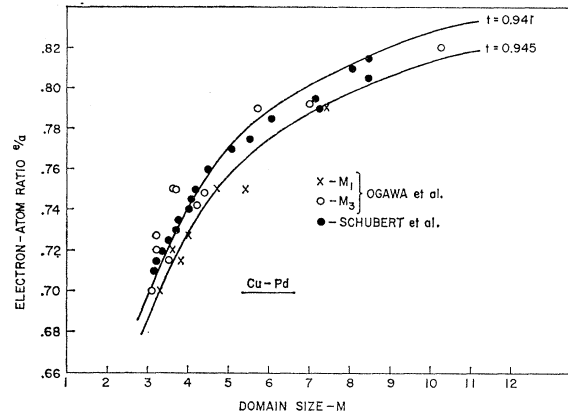


FIG. 7. Domain size M vs electron-atom ratio e/a for anti-phase structures in the Cu-Pd-alloy system.

boundaries, respectively. Since the separation in both directions is the same, the condition is exactly the same as that for the case of the AB -type alloy. Not only is the domain size predicted in the same way as the AB type, but the distortion of the lattice in the direction of the superperiod should also occur in the same way¹¹.

1. Cu-Pd System

Long-period superlattices have been found in the Cu-Pd system for Pd contents ranging from 20–30 at. %. From the electron diffraction work of Watanabe and Ogawa,³ and from x-ray investigations by Hirabayashi and Ogawa,¹² and Schubert *et al.*,¹³ a one-dimensional long-period superlattice has been found in the alloys having Pd contents from about 20 to 26 at. %. The two-dimensional structure is found at higher concentrations. The long-period superlattice forms in the $\mathbf{c}(\mathbf{a}_3)$ direction and has an antiphase of the first kind as defined by the “out-of-step vector” $\frac{1}{2}(\mathbf{a}_1 + \mathbf{a}_2)$. From the reported data, one can plot the accumulated data on domain size M vs the electron-atom ratio assuming a valence of one for Cu and zero for Pd. This is shown in Fig. 7. In this figure, the values for two-dimensional cases are also plotted, where M_3 should be taken as the period of the one dimensional superlattice, as referred to by Ogawa *et al.*,¹² as will be shown later. Since the e/a ratio is less than one, or more exactly less than the critical value of about 0.85 including the correction factor due to t , the stabilization should occur at the inner zone faces and consequently the negative sign in Eq. (9) must be used to calculate the theoretical curve. The calculated curve using a truncation factor $t = 0.941$ is shown in Fig. 7 and it can be seen that the agreement is very good.

¹¹ H. Sato and R. S. Toth, J. Phys. Soc. Japan, Supplement, 1962 (to be published).

¹² M. Hirabayashi and S. Ogawa, J. Phys. Soc. Japan 12, 259 (1957).

¹³ K. Schubert, B. Kiefer, M. Wilkens, and R. Haefler, Z. Metallk. 46, 692 (1955).

When the long-period superlattice is formed, the lattice contracts in the direction of the period so that the c/a ratio becomes less than one. This is the correct change predicted by the theory for an alloy where stabilization occurs at the inner-zone boundaries.

2. Cu-Pt System

A one-dimensional long-period superlattice is found in the Cu-Pt system at Pt contents around 25 at. %. Schubert *et al.*¹³ have determined the structure of this system using x rays and have found the period of the antiphase to lie in the c direction. Using their data and assuming a valence of one for Cu and zero for Pt, one can plot the domain size M vs e/a and compare it with the theoretical curve, using the minus sign and a truncation factor $t=0.958$ in the equation. This is shown in Fig. 8 where it is seen that the curve fits the data very well. When the superlattice is formed, the c/a ratio becomes less than one as the theory predicts.

3. Ag-Mg System

In the alloy range of 20 to 30 at. % Mg, there occurs a one-dimensional superlattice having an antiphase of the first kind. This structure was first suggested by Clarebrough and Nicholas^{14,15} and a definite structure was established from x-ray work of Schubert *et al.*¹³ and by Fujiwara *et al.*¹⁶ From this data one can plot the domain size M vs e/a assuming a valence of two for Mg and one for Ag. This is shown in Fig. 9, together with the theoretical curve. The curve was obtained from Eq. (9) using the plus sign and a value of $t=0.962$, and fits the data very well.

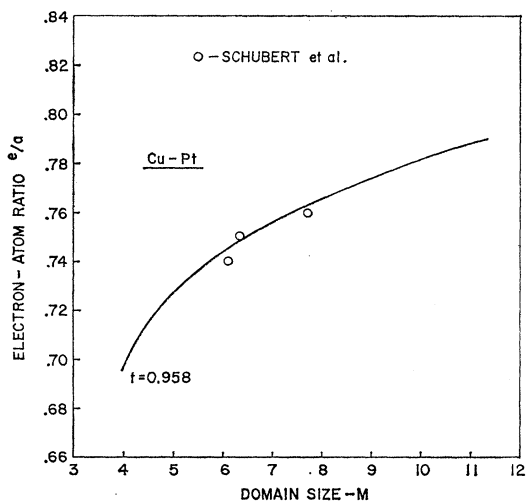


FIG. 8. Domain size M vs electron-atom ratio e/a for antiphase structures in the Cu-Pt-alloy system.

¹⁴ L. M. Clarebrough and J. F. Nicholas, Australian J. Sci. Research Ser. A 3, 284 (1950).

¹⁵ J. F. Nicholas, Proc. Phys. Soc. (London) A66, 201 (1953)

¹⁶ K. Fujiwara, M. Hirabayashi, D. Watanabe, and S. Ogawa, J. Phys. Soc. Japan 13, 167 (1958).

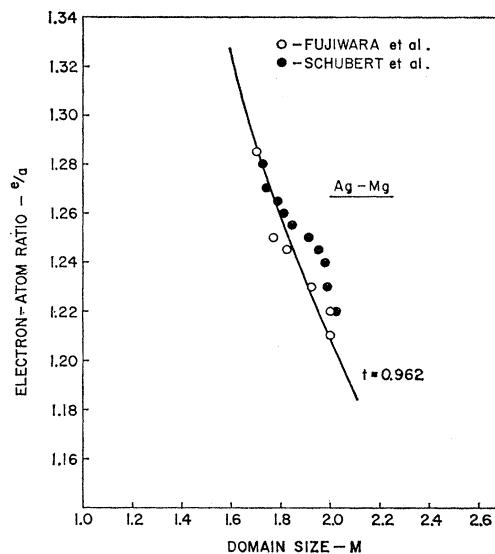


FIG. 9. Domain size M vs electron-atom ratio e/a for antiphase structures in the Ag-Mg-alloy system.

The alloys at these concentrations are cubic in the disordered state, but upon ordering and forming the long-period superlattice, distort and form a tetragonal structure with c/a greater than one. Since the period of the antiphase is in the c direction, this is the distortion predicted by the theory for alloys having e/a values greater than the critical value.

4. Au-Cd System

A one-dimensional long-period superlattice isomorphous with the structure of Ag_3Mg has been described by Schubert *et al.*¹³ and recently by Hirabayashi and Ogawa,¹⁷ using x-ray techniques. Only three compositions have been investigated, these being 24.6, 25.0, 25.5 at. % Cd. Assuming a valence of one for Au and two for Cd, one can plot M vs e/a for these three alloys. Using Eq. (9) with a plus sign and a value of $t=0.95$, one can compare the theoretical curve with these points as shown in Fig. 10. As pointed out by the authors, the domain size does not deviate from the value $M=2.0$. Very little change, if any, should occur since the e/a ratio of these alloys lie in a region where the e/a vs M curve is very steep. However, we cannot deny that there is a strong tendency for the alloy to stick to the value $M=2$ even if the e/a value indicates a smaller value for M . This tendency is observed not only in the Au-Cd system but also in the Ag-Mg system, the Au-Zn system and even in CuAu II with additional elements. In order to have a value M less than 2, the size of the antiphase domains would result from a mixture of $M=1$ and 2. Since the change from $M=2$ to $M=1$ would cause an especially large increase in the domain boundary energy, there should be a tendency for an alloy to avoid this change in structure.

¹⁷ M. Hirabayashi and S. Ogawa, Acta Met. 9, 264 (1961).

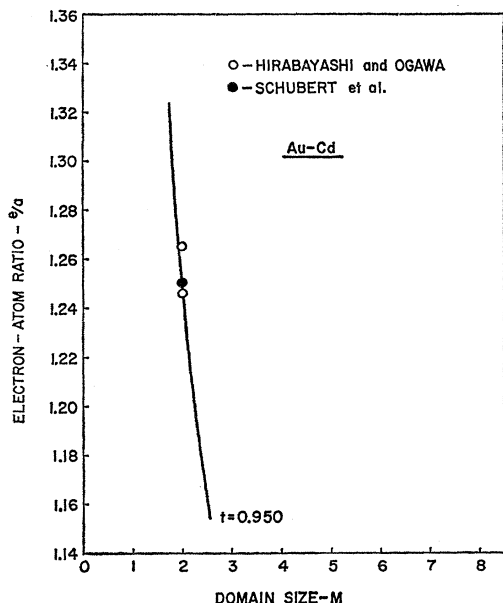


FIG. 10. Domain size M vs electron-atom ratio e/a for antiphase structures in the Au-Cd-alloy system.

The c/a ratio becomes greater than one when the antiphase structure is formed, as predicted for an alloy of this type.

5. Au-Zn System

Another antiphase structure isomorphous to Ag_3Mg and Au_3Cd is found in the Au-Zn system. This structure referred to as $\text{Au}_3\text{Zn(H)}$ is found only at high temperatures. Upon cooling, a more complicated orthorhombic structure is formed. Iwasaki *et al.*¹⁸ and Schubert *et al.*¹⁹ have found that the domain size is $M=2.0$ for compositions ranging from 20 to 29 at. % Zn. Assuming a valence of two for Zn, one can plot this data and compare with the theoretical curve based upon a value of $t=0.95$. This is shown in Fig. 11. The curve is quite steep and therefore the domain size should not deviate much, if at all, from the value $M=2.0$, as in the case of Au_3Cd .

As predicted by the model, the c/a ratio becomes larger than one for these alloys, when the antiphase structure is formed.

6. Cu-Au System

Quite recently the existence of an equilibrium Cu_3Au II phase at around 32 at. % Au has been reported in which a one-dimensional superlattice with a period $M=9.0$ is formed.^{19,20} One-dimensional antiphase domains have been reported previously in the Cu_3Au range

¹⁸ H. Iwasaki, M. Hirabayashi, K. Fujiwara, D. Watanabe, and S. Ogawa, *J. Phys. Soc. Japan* **15**, 1771 (1960).

¹⁹ R. E. Scott, *J. Appl. Phys.* **31**, 2112 (1960).

²⁰ S. Yamaguchi, D. Watanabe, and S. Ogawa (private communication).

by several researchers,^{21,22} but were assumed to occur as an intermediate phase since the domain size varied considerably with annealing and was quite large. The period of the domain in this equilibrium phase seems rather long from the view of the electron-atom ratio. However, in this system, the domain boundary energy is comparable to the stabilization energy,¹ and this value of M could be explained in terms of the effect of the domain boundary energy. A more detailed study would be required to determine the origin of the long period in this system.^{22a}

A summary of the pertinent data on one-dimensional long-period superlattices is given in Table I.

As is indicated in Figs. 7-11 and in Table I, the agreement of the theory with the experimental results is more than satisfactory if one thinks of the simpleness of the model adopted. The following features are especially important in the comparison of the theory with the experimental results:

(1) The dependence of the period M on the electron-atom ratio can be fitted by a theoretical curve with almost the same truncation factor t , which is about 0.95, in all alloy systems investigated.

(2) Both branches of the e/a vs M curves for alloy systems having e/a values greater or less than the critical value are explained.

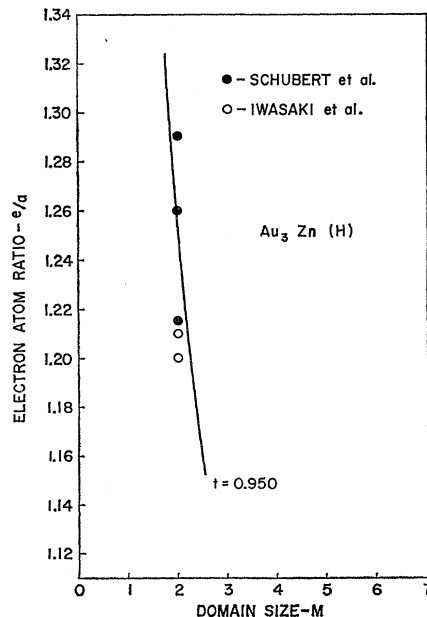


FIG. 11. Domain size M vs electron-atom ratio e/a for antiphase structures existing only at high temperatures in the Au-Zn-alloy system.

²¹ A. Guinier and R. Griffoul, *Rev. mét.* **55**, 387 (1948).

²² H. Raether, *Z. angew. Phys.* **4**, 53 (1952).

^{22a} Note added in proof. A detailed study of the Cu-Au system was carried out by the authors and the origin of the unexpectedly long period of Cu_3Au II was found to be due to the domain boundary energy. R. S. Toth and H. Sato, *J. Appl. Phys.* (to be published).

TABLE I. Summary of data on one-dimensional long-period superlattices.

Alloy series	Composition range (At. %)	Antiphase type	$e/a - (e/a)_c^a$	$(c/a) - 1$	Truncation factor t
Cu-Pd	20-26% Pd	first kind	—	—	0.941
Cu-Pt	24-26% Pt	first kind	—	—	0.958
Au-Cd	24.6-25.5% Cd	first kind	+	+	0.950
Ag-Mg	22-28% Mg	first kind	+	+	0.962
Au-Zn	21-29% Zn	first kind	+	+	0.950
Cu-Au	(a) CuAu II + additional elements	first kind	+	+ ^b	0.950
	(b) 31.6%	first kind	+

^a The critical value of the electron-atom ratio.

^b Here b/a is taken instead of c/a , since the c axis is taken for the tetragonal structure of CuAu I.

(3) The type of “out of step” at the antiphase boundary is correctly predicted by the theory.

(4) The tetragonal distortion of the lattice c/a , which depends on the e/a ratio, is correctly predicted by the theory.

These agreements of the theory with the experimental facts cannot be mere coincidence, and it can definitely be concluded that the Brillouin-zone mechanism discussed is the decisive origin for the alloy to choose a complicated periodic structure. The fact that the size of the Brillouin zone changes continuously with the change in the number of electrons so that it always contains a reasonable size of the Fermi sphere, indicates definitely that the stabilization takes place at the zone boundary.

As was pointed out in LPS I, there seems to be some question concerning the shape of the Fermi surface in alloys in applying the above idea to the stability of alloy phases. The recent study on the Fermi surface of noble metals (Cu, Au, Ag) indicates that the Fermi surface of these metals bulges out in the $[111]$ direction and touches the $\{111\}$ boundary.²³ It was pointed out in LPS I that this fact might not be compatible with the manner of interpretation for CuAu II and, more generally, with the application of Jones' model²⁴ to the prediction of the phase boundaries of alloys. However, this is not necessarily true. According to measurements, the diameter of the neck of the Fermi surface is rather small and, therefore, it leaves a reasonably spherical surface in the $[110]$ direction.²³ Therefore, the reduction in the energy of electrons at the $\{110\}$ boundary of the Brillouin zone is still possible. At the same time, the bulging out of the neck reduces the belly diameter, and this is equivalent to having a smaller Fermi sphere in the $[110]$ direction. In addition, the shape of the remaining Fermi surface is not quite spherical and is contracted somewhat in the $[110]$ direction.^{25,26} There should also be a distortion of

the Fermi surface at the zone boundary at contact, although the exact relation where the maximum stabilization takes place is not known. Thus, the fact that the truncation factor t we adopted to correct for the nonsphericity of the Fermi surface has a common value of 0.95 for many alloy series can be reasonably well explained with this idea.²⁷

This concept is not inconsistent with the case where the e/a value is low. Since the major energy gap nearest to the center of the Brillouin zone occurs across the $\{111\}$ boundary, there is a tendency for the Fermi sphere to bulge out in this direction, although it may not touch the $\{111\}$ boundary. Therefore, the effective diameter of the Fermi sphere in the $[110]$ direction will be affected as described above.

IV. TWO-DIMENSIONAL LONG-PERIOD SUPERLATTICES

It has been shown that a one-dimensional long-period superlattice for an A_3B -type alloy obtains its stabilization by the reduction in the energy of free electrons at eight of the twelve $\{110\}$ Brillouin-zone faces (two sets out of three sets of four Brillouin-zone faces each). Further stabilization could occur if all twelve faces of the zone were involved in a similar manner. This can be done by having one more superperiod in the direction perpendicular to the previous one. In this sense, a two-dimensional superstructure would be the more stable form of a long-period superlattice and, therefore, the one-dimensional superlattice can be assumed to be an intermediate phase while the three-dimensional superlattice should not occur at all.

The relative stability of each type of superstructure would depend on the energy balance between the increase in boundary energy as a result of the formation of antiphase boundaries, and the reduction in the energy of electrons at the Brillouin-zone faces. The introduction of the two-dimensional antiphase creates extra boundaries and therefore increases the boundary energy above that for the one-dimensional case.

²³ *The Fermi Surface, Proceedings of an International Conference at Cooperstown, New York* (John Wiley and Sons, Inc., New York, 1960).

²⁴ H. Jones, Proc. Roy. Soc. (London) **A144**, 225 (1934); **A147**, 396 (1934); Proc. Phys. Soc. (London) **49**, 250 (1937).

²⁵ R. W. Morse, in *The Fermi Surface*, edited by W. A. Harrison and M. B. Webb (John Wiley & Sons, New York, 1960) reference

23, p. 214; R. W. Morse, A. Myers and C. T. Walker, J. Acoust. Soc. Am. **33**, 699 (1961).

²⁶ B. Segall, Phys. Rev. Letters **7**, 154 (1961), Phys. Rev. **125**, 109 (1962); G. A. Burdick, Phys. Rev. Letters **7**, 156 (1961).

²⁷ H. Sato and R. S. Toth, Phys. Rev. Letters **8**, 239 (1962).

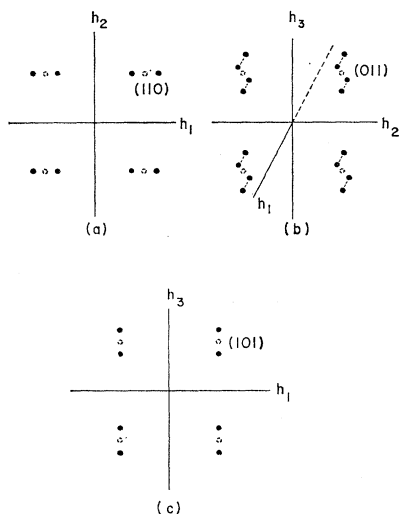


FIG. 12. Splitting of the (110) superlattice spots in the three principal planes for a two-dimensional long-period superlattice with a combination of an antiphase of the first kind and an antiphase of the second kind (*i* type). The third axis is added when it is necessary to show the separation in the direction perpendicular to the plane.

The shape of the Brillouin zone which results from the formation of a two-dimensional antiphase structure and therefore the reduction in energy depends upon the type of antiphase at the domain boundary as discussed for the one-dimensional superlattice case, where only an antiphase of the first kind is found. The relation is especially important in the two-dimensional case, because not only are two kinds of antiphase boundaries created in perpendicular directions, but also at least one set of four Brillouin-zone faces is doubly affected by the two-dimensional superperiod as will be explained later. Thus we may consider simultaneously the stabilization of these structures and the choice of antiphase at the two kinds of boundaries.

The following sets of antiphase boundaries are possible: both having an antiphase of the first kind; both having an antiphase of the second kind of the same type (either *i* or *e* type), there being two sorts of "out of steps" for the antiphase of the second kind; mixtures of the first and either type of the second kind and a mixture of the two different types of the second kind. Since the mixture of the first and second kind of out-of-step is usually found in the two-dimensional long-period structure, let us consider this case first to see if there is any advantage for this particular kind of mixture over others. The general manner of separation of spots can be calculated in a similar manner to that for the one-dimensional superlattice, although more complications arise.

The structure amplitude of the two-dimensional periodic superlattice based on Fig. 1(b) can be given by the following equation²⁸

²⁸ D. Watanabe, J. Phys. Soc. Japan 15, 1030 (1960).

$$|S| = \left| \frac{\sin \pi N_1 (2M_1) A_1}{\sin \pi (2M_1) A_1} \right| \left| \frac{\sin \pi M_1 A_1}{\sin \pi A_1} \right| \left| \frac{\sin \pi N_2 A_2}{\sin \pi A_2} \right| \\ \times \left| \frac{\sin \pi N_3 (2M_3) A_3}{\sin \pi (2M_3) A_3} \right| \left| \frac{\sin \pi M_3 A_3}{\sin \pi A_3} \right| |\Phi|, \quad (10)$$

where

$$\Phi = \Phi_I + \Phi_{II} \exp(2\pi i M_3 A_3) + \Phi_{III} \exp(2\pi i M_1 A_1) \\ + \Phi_{IV} \exp[2\pi i (M_3 A_3 + M_1 A_1)].$$

The meaning of the variables A_i and N_i is as given before. The relations among the structure factors Φ_I , Φ_{II} , Φ_{III} and Φ_{IV} are determined from the relations of antiphase structures among them. If the antiphase in the A_3 direction is of the first kind and that in the A_1 direction is of the second kind (*i* type), these structure factors are given as follows:

$$\Phi_I = E_A \{1 + \exp[\pi i (A_1 + A_2)] + \exp[\pi i (A_2 + A_3)]\} \\ + E_B \exp[\pi i (A_3 + A_1)], \\ \Phi_{II} = E_A \{1 + \exp[\pi i (A_1 + A_2)] + \exp[\pi i (A_3 + A_1)]\} \\ + E_B \exp[\pi i (A_2 + A_3)], \\ \Phi_{III} = E_A \{ \exp[\pi i (A_1 + A_2)] + \exp[\pi i (A_2 + A_3)] \\ + \exp[\pi i (A_3 + A_1)] \} + E_B, \\ \Phi_{IV} = E_A \{1 + \exp[\pi i (A_2 + A_3)] + \exp[\pi i (A_3 + A_1)]\} \\ + E_B \exp[\pi i (A_1 + A_2)].$$

Now, for superlattice spots (011), for example, we would like to show that it splits into four for such a two-dimensional long-period superlattice described above. Exactly as before, with little sacrifice in approximation when M_1 and M_3 are both reasonably large, the manner of splitting of this spot can be calculated for (011) with Eq. (10),

$$\Phi = (E_A - E_B) [1 - \exp(2\pi i M_1 \delta_1)] \\ \times \{1 - \exp[2\pi i M_3 (1 + \delta_3)]\}, \quad (12)$$

$$|\Phi| = |(E_A - E_B)| |2[1 - \cos(2\pi M_1 \delta_1)]| \\ \times |2\{1 - \cos[2\pi M_3 (1 + \delta_3)]\}|.$$

Therefore, the maximums appear when

$$\delta_1 = \pm n_1 / 2M_1 \quad \text{and} \quad \delta_3 = \pm n_3 / 2M_3 \quad (13)$$

are satisfied, where n_1 and n_3 are both odd integers. The primary separation (for $n_1 = n_3 = 1$) of (011) is therefore into four spots ($\pm 1/2M_1, 1, 1 \pm 1/2M_3$).

In exactly the same way, the spots (101) and (110) are proved to split into two along h_3 and h_1 , respectively. Generally speaking, superlattice spots separate in the direction of the period in such a manner when the index h_i and h_k mix if the "out-of-step" shift is $\pm \frac{1}{2}(\mathbf{a}_i + \mathbf{a}_k)$. When the double splitting occurs as in Eq. (13) due to a two-dimensional superperiod, the one spot splits into four instead of two. In other words, the manner of separation is determined by the type of antiphase structure of the particular alloy.

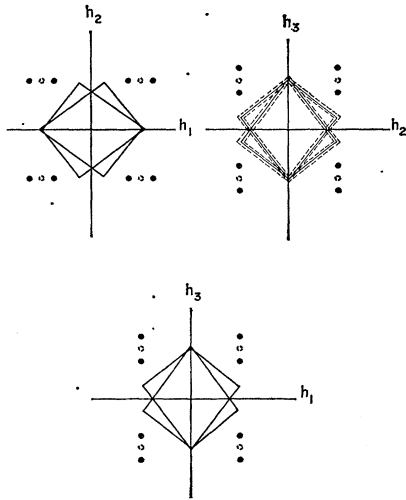


FIG. 13. Cross sections of the Brillouin zone for the case shown in Fig. 12. The dotted lines in the h_2 - h_3 plane indicate the tilting of the Brillouin-zone surfaces corresponding to the separation of the superlattice spots in the direction perpendicular to the plane. The h_1 axis is not added here.

The approximate calculation adopted above is reasonably good as long as the M 's are reasonably large. However, if the M 's become smaller, the intensity of the second maximums, which are not the maxima determined by Eq. (13), for example, becomes appreciable and a more detailed calculation is required especially for a complex separation of spots such as doubly split spots.

If we choose the direction perpendicular to the first-kind antiphase to be in the direction of \mathbf{a}_3 and that perpendicular to the second-kind antiphase to be in \mathbf{a}_1 , the out-of-step vector for the former is $\frac{1}{2}(\mathbf{a}_1 + \mathbf{a}_2)$ and, for the latter, is chosen to be $\frac{1}{2}(\mathbf{a}_1 + \mathbf{a}_3)$ (i type). The other possibility for the second kind (e type) is $\frac{1}{2}(\mathbf{a}_1 + \mathbf{a}_2)$ but these two are not equivalent when the combination with other types of antiphase is treated as indicated before. The latter case will be discussed later. In Fig. 12, the manner of separation of the $\{110\}$ superlattice spots is shown for the former kind of combination of the antiphases in each principal plane, \mathbf{h}_1 - \mathbf{h}_2 , \mathbf{h}_2 - \mathbf{h}_3 , \mathbf{h}_3 - \mathbf{h}_1 in the reciprocal lattice. Let us further specify the separation of the superlattice spots in the \mathbf{h}_3 direction as δ_3 , and in the \mathbf{h}_1 direction as δ_1 . The manner of separation of the $\{110\}$ Brillouin-zone faces which corresponds to the separation of the superlattice spots is shown in Fig. 13. The distances from the center of the Brillouin zone to these faces are

$$\begin{aligned} (2 \pm 2\delta_1 + \delta_1^2)^{\frac{1}{2}} & \quad \text{for } \mathbf{h}_1\text{-}\mathbf{h}_2 \text{ groups (a),} \\ (2 \pm 2\delta_3 + \delta_3^2 + \delta_1^2)^{\frac{1}{2}} & \quad \text{for } \mathbf{h}_2\text{-}\mathbf{h}_3 \text{ groups (b),} \\ (2 \pm 2\delta_3 + \delta_3^2)^{\frac{1}{2}} & \quad \text{for } \mathbf{h}_3\text{-}\mathbf{h}_1 \text{ groups (c).} \end{aligned} \tag{14}$$

The plus and minus signs correspond to outer and inner zone boundaries as before. Note that the (b) group of faces is doubly affected.

It is easily understood, from the above conditions, that there is no way of inscribing one sphere to all the separated Brillouin-zone boundaries as was done in the one-dimensional case. To find the condition for the maximum reduction in energy, it is necessary to obtain detailed information about the electronic structure of the alloy, i.e., the energy contour, energy gap at the boundary, etc. Since the separations are equal in the case of the one-dimensional superlattice, it was possible to avoid this intricate situation. Because such information is hard to get at the present stage, let us instead try to determine the minimum energy condition here from the condition of the best possible fit of the Fermi sphere to the Brillouin-zone faces. Then the condition (b) of Eq. (14) should first be chosen as the radius of the Fermi sphere. As mentioned previously, a one-dimensional superperiod affects eight of the twelve Brillouin zone-faces (two sets of three sets of Brillouin-zone faces), and consequently, at least one set of faces is doubly affected when a two-dimensional superlattice is formed. This is indicated by condition (b). The double effect which occurs for the initial four faces of the zone results in a tilting of the final zone faces in two directions in addition to the splitting. Thus the number of Brillouin-zone faces resulting from condition (b) for either the inner or outer set would be eight instead of the usual four. Because we are dealing with the stabilization at the zone boundary and, for this, the number of boundaries which contact the Fermi sphere should play a decisive role, one would expect condition (b) to be met whenever a two-dimensional superperiod of this kind is formed. A combination of fitting to condition (b) plus one of the other two conditions would then provide the maximum stabilization. This can only be done by the condition that the distance given by (b) and that by (a) are equal, since the distance given by (c) is always shorter than that given by (b). In order that the distances be equal, the following condition should be met:

$$2 \pm 2\delta_3 + \delta_3^2 + \delta_1^2 = 2 \pm 2\delta_1 + \delta_1^2, \tag{15}$$

or

$$\pm 2\delta_3 + \delta_3^2 = \pm 2\delta_1.$$

Therefore, δ_1 should be larger than δ_3 if we take the plus sign and vice versa, and the value of δ_3 (or δ_1) can be determined from the e/a value using an equation equivalent to Eq. (9),²⁹ with a truncation factor which is assumed to be the same for the two directions. The important conclusion here is that the domain sizes should be different in the two directions and that their values depend upon the e/a value.

If we take the "out of step" for the second kind to be $\frac{1}{2}(\mathbf{a}_1 + \mathbf{a}_2)$ (e type) instead of $\frac{1}{2}(\mathbf{a}_1 + \mathbf{a}_3)$, the manner of separation of the $\{110\}$ superlattice spots and consequently the separation of the $\{110\}$ Brillouin-zone surfaces will be different from above and will be as shown in Fig. 14. It is clear from Figs. 13 and 14 that

²⁹ The choice of taking δ_3 or δ_1 will be discussed later.

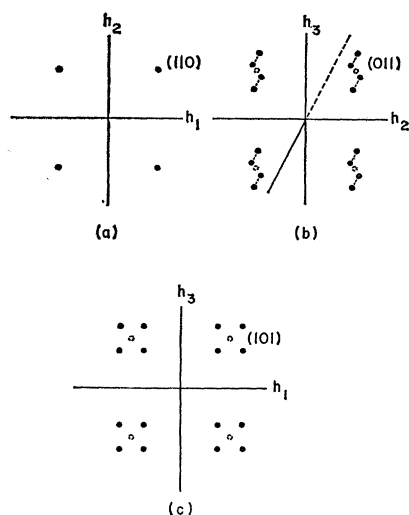


FIG. 14. Splitting of the (110) superlattice spots in the three principal planes for a combination of an antiphase of the first kind and an antiphase of the second kind (*e* type). Note that the (110) spots are not affected. For such a case, a three dimensional structure may be conceivable.

the Fermi sphere cannot be accommodated within the Brillouin zone in the latter case as well as in the former case. Therefore, this kind of "out of step" is energetically less favorable and this means that if the combination of the first and second kind should appear, only the former combination should be the right one.

The manner of splitting of the superlattice spots for the combination of two first kinds of "out of step" and for the combination of the two second-kind antiphases of the same type are given in Figs. 15–17. A combination of an *e* type and *i* type second-kind antiphase gives a manner of splitting shown in Fig. 18. It is easily seen that none of these combinations of antiphase give a better fit to a single Fermi sphere than the combination

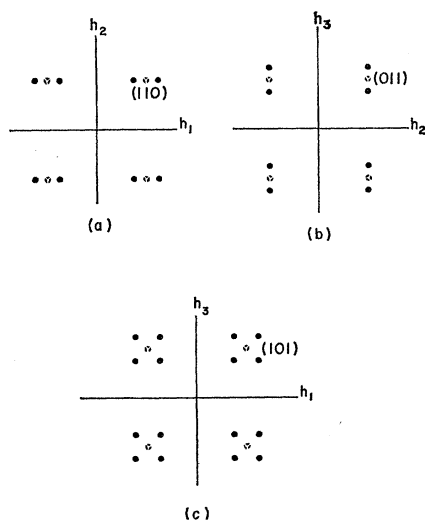


FIG. 15. Splitting of the (110) superlattice spots in the three principal planes for a combination of two first kind of antiphases.

of the first and the second kind of antiphase (*i* type), as long as the values of δ_3 and δ_1 are small. In this sense, it can be concluded that whenever a two-dimensional antiphase structure appears, the combination of the first and the second kind "out of steps" (*i* type) should be formed at the antiphase boundaries as long as δ_3 and δ_1 remain reasonably small or the e/a value of the alloy is reasonably near the critical value.

Although the combination of the antiphases of the first and second kind first given, meets reasonably well the condition for stabilization as long as δ_3 and δ_1 are small, the difference in distance between the condition (b) and (c) in Eq. (14) becomes larger as δ_3 and δ_1 become larger. Therefore, the condition for the stabilization of this structure becomes worse as δ_3 and δ_1 become larger. In such a case, a reasonable conclusion cannot be drawn without a detailed knowledge of the electronic structure. At the same time, the manner of

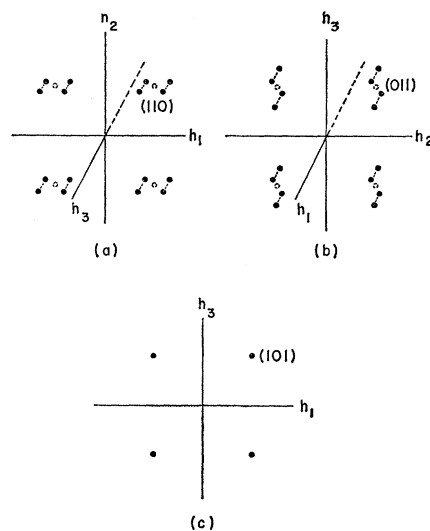


FIG. 16. Splitting of the (110) superlattice spots in the three principal planes for a combination of two *i*-type second-kind antiphases.

separation of the spots based on the calculated intensity as given here is not valid when the period becomes shorter and a detailed calculation is required. The inequality in the distances from the center to the separated Brillouin-zone boundaries in different directions could be adjusted to some extent by a distortion of the lattice. A distortion of this origin should also exist in a two-dimensional structure. However, when e/a becomes large and the deviation becomes accordingly large, the cost in energy that the alloy should pay for the distortion to accommodate the Fermi sphere in a perfect way is, of course, too large. Instead, the energy required to introduce new types of antiphase boundaries, if there is any possible way, would be less. In this sense, it is possible that, as e/a increases, the combination of the antiphase for two-dimensional long-period super-

lattices changes from the combination of the first and the second kind to some other combination given above, to other directions of the superperiod from the (100) direction or to a different complicated antiphase structure. This seems to explain the appearance of complicated structures in the case of Au-Mn and Au-Zn alloys as shown later.

The condition for the distortion of the lattice when forming the two-dimensional long-period superlattice is relatively simple for the case of the mixture of the first- and second-kind antiphase boundaries. From the shape of the Brillouin zone [Fig. 5(b)] and the manner of separation of the Brillouin zone of Fig. 13 it is easily understood that the adjustment for the force exerted by the Fermi surface to the boundary is taken care of by the single deformation of the zone along the h_3 direction, which is the direction of the period with the first-kind antiphase. From the geometry, only one pair

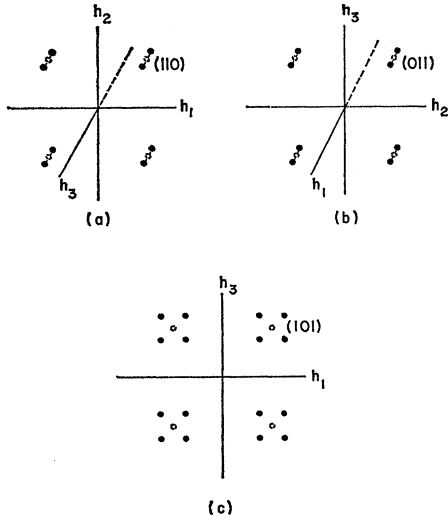


FIG. 17. Splitting of the (110) superlattice spots in the three principal planes for a combination of two *e*-type second-kind antiphases.

of apexes along the h_3 axis of the Brillouin zone remains practically unseparated and the distortion along this axis changes the separation of both directions. Therefore, in such a superlattice, the distortion is practically tetragonal except for the further minor distortion indicated above and therefore the condition for the distortion is the same as in the one-dimensional superlattice. Thus, the c/a ratio is determined by the value of the electron-atom ratio. In all other cases, such a simple condition does not hold and the distortion should be orthorhombic.

Observations on several two-dimensional long-period superlattices have been reported, among which the research in the Cu-Pd system is the most systematic.^{3,12} The two-dimensional antiphase structure is found to exist at Pd concentrations from about 26 to 30 at. %. The concentration at which the one-dimensional struc-

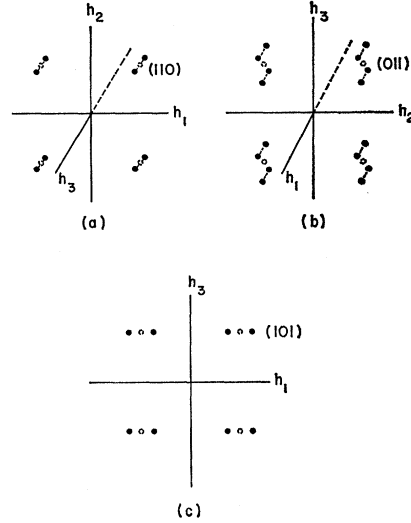


FIG. 18. Splitting of the (110) superlattice spots in the three principal planes for a combination of an *e*-type and *i*-type second-kind antiphase.

ture changes to the two-dimensional one seems to depend on whether the sample is a film or a bulk. At the same time, there seems to be some difference in the value of the domain size between the two cases. However, these values are treated here without any discrimination. The plot of e/a vs M for the two domains is shown in Fig. 7, where M_3 represents the domain size in the direction having an antiphase of the first kind and M_1 represents the domain size in the direction having an antiphase of the second kind. The points fit quite

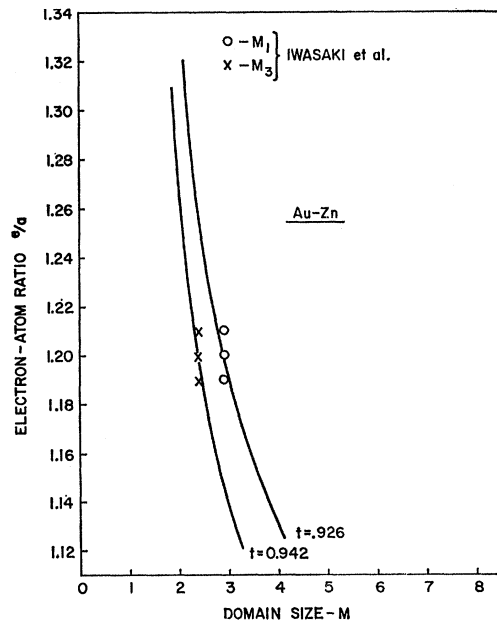


FIG. 19. Domain size M vs electron-atom ratio e/a for the two-dimensional antiphase structures in the Au-Zn-alloy system. The truncation factors shown are from an independent fitting of Eq. (9) to the two periods M_1 and M_3 .

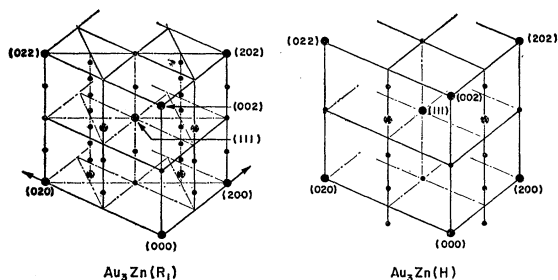


FIG. 20. The reciprocal lattice of $\text{Au}_3\text{Zn}(H)$ and $\text{Au}_3\text{Zn}(R_1)$ according to Iwasaki *et al.*⁷ The encircled spots indicate the corresponding Brillouin-zone boundaries which enclose the Fermi sphere.

well on the theoretical curve obtained from Eq. (9) using a value of $t=0.945$ or 0.941 as shown. However, as pointed out before, there is an ambiguity as to whether δ_3 or δ_1 should be used to determine the relation between e/a and the period in a relation such as Eq. (9). In the case of the one-dimensional superlattice, the antiphase of the first kind always appears. In the Cu-Pd system, M_3 in the one-dimensional case at lower concentration of Pd continues smoothly to M_3 of the two-dimensional superlattice at higher concentration of Pd. In this sense, δ_3 , instead of δ_1 , should give the radius of the Fermi sphere and should be taken to get a relation between e/a and M . However, since the truncation factor should be different for the two directions h_3 and h_1 , it does not seem to be necessary to lay too much weight on this kind of matter. Using Eq. (11), we can calculate the domain size M_1 from M_3 and compare with the experimental data. The results are shown in Table II, and it can be seen that the calculated values agree reasonably well with the data, especially in the sense that M_3 is larger than M_1 which is in accord with the theoretical prediction. The lattice distorts tetragonally even when the two-dimensional antiphase is formed and c/a is less than one for these alloys. This also agrees with the theoretical prediction.

In the Au-Zn system, a two-dimensional antiphase structure is found near Au_3Zn , in which a mixture of an antiphase of the first and the second kind exists.¹⁸ As shown in Fig. 19, the relation between M and e/a is best fit by a theoretical curve with a reasonable value of t . The lattice distorts tetragonally and its c/a ratio is larger than one as expected from the theory. However, in this system, the size difference for δ_3 and δ_1 is just contrary to the theoretical expectation. In other words, M_3 is larger than M_1 just as in the case of Cu-Pd alloys, irrespective of that fact that the e/a of this system is larger than the critical value. Since the boundary energy affects the size of the domains, this fact may indicate that there is a difference in boundary energy for the first and the second kind antiphase. At higher Zn content, a complicated antiphase structure $\text{Au}_3\text{Zn}(R)$ appears.¹⁸ The relation of this complicated structure to an ordinary antiphase structure can be visualized

TABLE II. Calculated value of the domain size M_1 from the observed values of M_3 based on Eq. (14) compared to observed values for the Cu-Pd system.

At. % Pd	M_1 (experimental)	M_1 (calculated)
21	7.4	6.07
25	4.7	3.87
27.3	4.0	3.47
28	3.6	3.47
28.5	3.8	3.84
30	3.3	3.38

by the comparison of the reciprocal lattice of $\text{Au}_3\text{Zn}(H)$ and $\text{Au}_3\text{Zn}(R_1)$,⁷ $\text{Au}_3\text{Zn}(H)$ being the high-temperature phase with a one-dimensional long-period structure (Fig. 20). The reciprocal lattice points which correspond to the Brillouin-zone boundaries enclosing the Fermi sphere are encircled by dotted lines. The additional 16 Brillouin-zone boundaries which correspond to the two additional encircled points of $\text{Au}_3\text{Zn}(R_1)$ in the figure enclose the Fermi sphere quite well along with the original eight Brillouin-zone boundaries of $\text{Au}_3\text{Zn}(H)$. From the calculation, the condition is found to be most suitably satisfied for alloys with e/a ratios which correspond to a period M slightly larger than two, agreeing with the experimental data. The $\text{Au}_3\text{Zn}(R_1)$ structure can be achieved by a slight shift of certain atoms from the equilibrium positions in the face centered cubic lattice along with an antiphase structure as shown in Fig. 21.³⁰ The transition from a usual antiphase structure to such a complicated structure can occur if the energy which accompanies this atomic shift is compensated by the reduction in energy of electrons. In any case, the appearance of such a complicated structure agrees with the general theoretical expectation.

In the Au-Mn system, a two-dimensional antiphase of very short period is found at Au_3Mn .²⁸ It has been interpreted that the antiphases are both of the first kind. In order to fit the theoretical curve to the actual

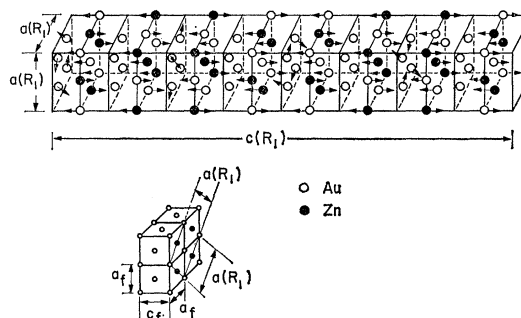


FIG. 21. The ordered structure of $\text{Au}_3\text{Zn}(R_1)$ according to Iwasaki.³⁰ Arrows show the directions of the atom shifts. The relation between the large unit cell and the fundamental unit cell is also shown. $a(R_1)$ and $c(R_1)$ indicate the unit cell length of $\text{Au}_3\text{Zn}(R_1)$ and a_f and c_f are those of the original face-centered cubic cells.

³⁰ H. Iwasaki, J. Phys. Soc. Japan 14, 1456 (1959).

TABLE III. Summary of data on alloy systems having two-dimensional antiphase structures.^a

Alloy series	Composition range	$e/a - (e/a)_c$	Antiphase type	M_1		M_3		$(c/a) - 1$	$(b/a) - 1$
				Truncation ^b factor	Antiphase type	Truncation ^b factor	Antiphase type		
Cu-Pd	26-30% Pd	-	second kind	0.945	first kind	0.941	-		
Au-Zn	19-21% Zn	+	second kind	0.926	first kind	0.942	+		
Au-Mn	25% Mn	+	first kind	1.026	first kind	0.939	+		+

^a c and b refer to the lattice constants of the unit cell in the direction of the period in order to use a conventional way of indicating the distortion. In a rigorous way, they should be written as a_3/a_2 and a_1/a_2 .

^b Truncation factors obtained from the independent fitting of Eq. (9) to the two domain sizes.

domain size, one must adopt, for one direction, a t value which is higher than the usual value of 0.95, (Fig. 22). At higher Mn contents, a more complex antiphase structure with noncrystallographic period and direction has been found.³¹ Since we can give a valence of two to manganese ions in the gold matrix, as to Zn ions, these facts, along with the Au-Zn alloys, appear to agree with a general theoretical expectation that the discrepancy from a standard antiphase structure should appear at high e/a values (or for large δ_3 and δ_1). The details of the interpretation concerning such complicated structures will be given in a future report. The distortion of the lattice in such complicated structures is an orthorhombic one and also agrees with the theoretical expectation. The fact that this distortion is an elongation in the direction of the period for both Au-Mn and Au-Zn seems to indicate that a similar stabilization mechanism is also operative in these complicated structures. Results on two-dimensional antiphase structures are summarized in Table III.

SUMMARY

The theory which had been developed to explain the origin of the long-period superlattice CuAu II was applied to explain similar one-dimensional and two-dimensional long-period superlattices in A_3B -type alloys.

In one-dimensional superlattices, although the situation is similar, there is an essential difference between an AB -type superlattice like CuAu II and an A_3B -type superlattice. The difference exists in the Brillouin-zone structure since the atomic arrangement of the A_3B type is cubic in contrast to the tetragonal symmetry of the AB -type alloy. Because of this fact, two kinds of antiphase boundaries can appear in an A_3B -type alloy. However, it was found that the "out of step" of the first kind which is the same as that observed in CuAu II was energetically more favorable. In this sense, all the discussions on A_3B -type alloys are parallel to the discussions on AB -type alloys and the size of the domains as well as the distortion at the formation of the long-period superlattice can be predicted with the use of the same argument as that for CuAu II. The theory provides a good explanation for all the phenomena characteristic to the one-dimensional long-period superlattice of

A_3B -type alloys observed so far. In this sense, the interpretation based on the Brillouin-zone structure of alloys should be regarded to be true. It is also indicated that the recent results concerning the shape of the Fermi surface of noble metals can be compatible with the stabilization mechanism of the long period superlattice.

The introduction of the additional superperiod to form a two-dimensional long-period superlattice gives the possibility of having a better accommodation for the Fermi sphere, all Brillouin-zone surfaces being adjusted. However, since this adjustment cannot be equal for three directions, the adjustment cannot be perfect. This causes further complications to the problem when e/a increases. Generally speaking, the application of the theory to the case of the two-dimensional long-period superlattice is far more complicated and the unique solution similar to that found in the one dimensional case cannot be obtained. For these, a detailed knowledge of the electronic structure of alloys is required, which in the case of the one-dimensional structure, can be avoided except in special problems. However, the theory still provides a reasonably good explanation of this compli-

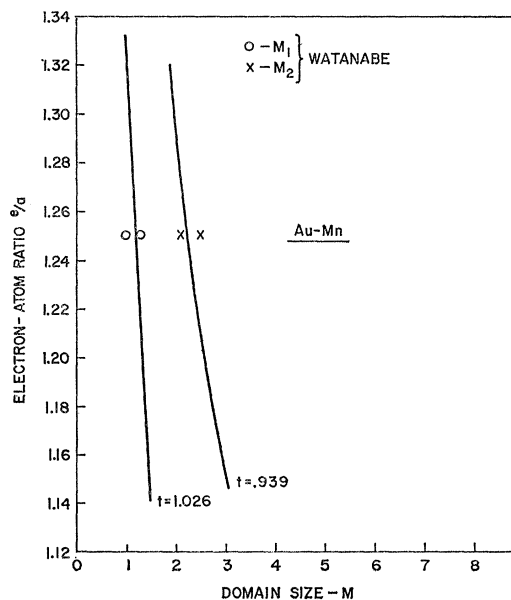


FIG. 22. Domain size M vs electron-atom ratio e/a for the two-dimensional antiphase structure in the Au-Mn-alloy system.

³¹ M. Tournarie, Sendai Symposium on Electron Diffraction, October, 1961 (unpublished), (private communication).

cated structure. It was found that a combination of the first kind and the second kind of out-of-step for the antiphase boundaries for respective directions was favorable as long as the domain size was not too small. In this case, the lattice distorts tetragonally and the sign of $(c/a)-1$ can be predicted from the electron-atom ratio as in the one-dimensional case. Also it was predicted that the domain size in two directions should be somewhat different. If the electron-atom ratio deviates much from the critical value and the domain size becomes smaller, the structure begins to be unstable and structures with other combinations of antiphase or more complicated structures can appear. In such a case, the lattice usually distorts orthorhombically. It is also proved that the three-dimensional antiphase structure should not occur.

Thus far, most of the properties of long-period superlattices can be satisfactorily explained from a very simple model concerning the Brillouin-zone structure

of alloys. The advantage of the present problem, which is reflected by the above results, is that the difference between very similar structures are being compared and therefore the change of a very small part of an energy term can be compared, keeping other energy terms almost constant. The quantitative agreement of the theoretical prediction with the experimental results justifies the fundamental assumption that the stabilization takes place at the Brillouin-zone boundary. However, the lack of exact theoretical knowledge concerning this point is felt in the treatment of the two-dimensional long-period superlattice as was shown. This situation limits the more detailed treatments of the problem.

ACKNOWLEDGMENTS

The authors wish to express their appreciation to Dr. A. Arrott for his critical reading of the manuscript and to Dr. A. W. Overhauser for his discussions.